Agenzia nazionale per le nuove tecnologie,
l'energia e lo sviluppo economico sostenibile

MINISTERO DELLO SVILUPPO ECONOMICO

Ricerca di Sistema elettrico

Sviluppo di un Modello LES per Fiamme Turbolente Premiscelate

E. Giacomazzi, D. Cecere, F.R. Picchia, N. Arcidiacono

Report RdS/PAR2013/255

SVILUPPO DI UN MODELLO LES PER FIAMME TURBOLENTE PREMISCELATE

E. Giacomazzi, D. Cecere, F.R. Picchia, N. Arcidiacono, (ENEA, UTTEI-COMSO)

Settembre 2014

Report Ricerca di Sistema Elettrico
Accordo di Programma Ministero dello Sviluppo Economico – ENEA
Piano Annuale di Realizzazione 2013
Area: Produzione di energia elettrica e protezione dell'ambiente
Progetto: B.2 - Cattura e sequestro della CO2 prodotta dall'utilizzo di combustibili fossili
Obiettivo: Parte A - b - Tecnologie per l'ottimizzazione dei processi di combustione
Task b.1 - Metodologie numeriche avanzate per la simulazione dei processi di combustione e la progettazione di componenti
Responsabile del Progetto: Stefano Giammartini, ENEA

Indice

Sommario

Nella precedente annualitá é stato sviluppato un nuovo modello di sottogriglia per Large Eddy Simulation (LES) per trattare l'interazione turbolenza/combustione in fiamme premiscelate. Questo modello ha l'ambizione di cogliere a livello locale (nello spazio) i diversi regimi di combustione stimando la frazione di volume reagente all'interno di ogni singola cella di calcolo in funzione del valore assunto da numeri caratteristici rappresentativi della fisica in gioco, come i numeri di Reynolds, Prandtl e quello di Damkhoeler. L'espressione finale di questa frazione dipende dal rapporto tra la velocita di propagazione turbolenta del fronte di fiamma e quella laminare, e dallo spessore del fronte di fiamma. Queste due fondamentali grandezze sono modellate diversamente in funzione del regime di combustione in cui la cella reagente viene a trovarsi. Sono anche considerati gli effetti di diffusione preferenziale delle specie combustibili piú leggere, come l'idrogeno, sulla propagazione del fronte nelle regioni del flusso caratterizzate da bassi livelli di stiramento fluidodinamico. Oltre a considerare l'effetto positivo delle diverse scale turbolente sulla combustione, dovuto all'aumentato mescolamento ed eventuale inspessimento del fronte, il modello considera anche gli effetti negativi in termini di estinzione localizzata, dovuta allo stiramento del fronte di fiamma da parte dei vortici di piccola scala. Il nuovo modello é stato validato, nel corso di questa annualit, mediante un caso test preventivamente definito e simulato dagli stessi autori con tecnica DNS (Direct Numerical Simulation). Il caso consiste in una fiamma premiscelata metano/idrogeno/aria relativa ad un bruciatore con tre iniettori a sezione rettangolare affiancati. La miscela fresca reagente (con 20% in volume di contenuto di idrogeno) esce dall'iniettore centrale, mentre dai due restanti iniettori esce a velocit ridotta una miscela costituita dai gas prodotti dalla combustione della miscela centrale. I risultati della DNS sono stati analizzati con dettaglio e costituiranno un importante database nel panorama internazionale. La simulazione LES con il modello LTSM sviluppato é stata confrontata con i risultati di riferimento offerti dalla DNS in termini di grandezze medie e fluttuazioni rms. Si riportano alcuni confronti significativi.

1 Introduction

A synthetic way to look at turbulence / combustion interaction consists in mapping what are possible combustion regimes. In fact, due to the complexity of multi-scale interaction between turbulence and chemistry, several combustion regimes may occur. Regime determination, i.e., the identification of the spatial structure and morphology of the reacting flow, is important for combustion modelling. Combustion regimes have been theoretically investigated for many years in premixed combustion [1, 2, 3, 4, 5, 6, 7, 8] by simply assuming the turbulence integral length scale, L, the associated turbulent velocity fluctuation, u'_{rms}, the laminar flame speed, S_L, and the flame front thickness, δ_F, all defined or measured in some way, as the main quantities characterizing the turbulence - chemistry interaction.

Typically, combustion regimes are mapped in two dimensional diagrams showing regions where the flow structure will feature flamelets, pockets or distributed reaction zones. Just as typically, these diagrams do not include the effect of important flame physics such as heat losses, flame curvature, viscous dissipation and transient dynamics, all affecting quenching. Furthermore, the effect of the Lewis number on quenching produced by stretching is not considered [9, p. 56-59].

1.1 Modelling the Favre Filtered Chemical Source Term

The Favre filtered chemical source term in the energy and single species transport equations is here modelled as $\widetilde{\omega}_i \approx \gamma^* \omega_i^*$, γ^* and ω_i^* being the local reacting volume fraction of the computational cell and the reaction rate of the $i-th$ chemical species, respectively.

The local reacting volume fraction is defined as $\gamma^* = \mathcal{V}_\mathcal{F}{}^*/\mathcal{V}_\Delta$, $\mathcal{V}_\mathcal{F}{}^*$ and $\mathcal{V}_\Delta$ being the reacting and the total volumes of the computational cell. In particular, the suggested Localized Turbulent Scales Model (LTSM) estimates the local reacting volume fraction γ^* assuming that a flame front having a surface area $\mathcal{A}_\mathcal{F}$ and thickness δ_F is contained in a computational cell volume of characteristic size $\Delta = \mathcal{V}_\Delta^{1/3}$, i.e.,

$$\gamma^* = \frac{\mathcal{V}_\mathcal{F}{}^*}{\mathcal{V}_\Delta} \approx \frac{\mathcal{A}_\mathcal{F}\delta_\mathcal{F}}{\mathcal{V}_\Delta} \approx \frac{\mathcal{S}_\mathcal{T}}{\mathcal{S}_\mathcal{L}}\mathcal{A}_\mathcal{L}\frac{\delta_\mathcal{F}}{\mathcal{V}_\Delta} \approx \frac{\mathcal{S}_\mathcal{T}}{\mathcal{S}_\mathcal{L}}\Delta^2\frac{\delta_\mathcal{F}}{\Delta^3} = \frac{\mathcal{S}_\mathcal{T}}{\mathcal{S}_\mathcal{L}}\frac{\delta_\mathcal{F}}{\Delta}\,. \tag{1.1}$$

This expression has been obtained with two main assumptions. The first is that within a wrinkled flame front the iso-surfaces of the progress variable are parallel [10]. The second assumption is that the ratio between the turbulent and the laminar flame surface areas scales as the ratio between the associated flame speeds , i.e., $\mathcal{A}_\mathcal{F}/\mathcal{A}_\mathcal{L} \equiv \mathcal{A}_\mathcal{T}/\mathcal{A}_\mathcal{L} \approx \mathcal{S}_\mathcal{T}/\mathcal{S}_\mathcal{L}$. With this modeling, subgrid flame front wrinkling and curvature effects are synthesized in this ratio. It is reminded that the laminar flame speed can be estimated as $\mathcal{S}_\mathcal{L} \approx (\alpha/\tau_{ch})^{1/2}$, the laminar flame thickness as $\delta_\mathcal{L} \approx (\alpha\,\tau_{ch})^{1/2}$, and that these two expressions imply $\frac{\delta_\mathcal{L}\mathcal{S}_\mathcal{L}}{\alpha} = 1$ The quantity $\alpha = k/(\rho C_p)$ is the thermal diffusivity, with k being the thermal conductivity, ρ the density and C_p the specific heat at constant pressure.

It is observed that the local flame at the base of Eqn. (1.1) may be laminar or turbulent, wrinkled or not, thickened by turbulence or not, depending on the local conditions of the flow. In particular, for a local laminar (planar) flame Eqn. (1.1) reduces to $\gamma^* \approx \delta_\mathcal{F}/\Delta$. When combustion is locally volumetric, $\gamma^* = 1$. Equation (1.1) refers to a laminar or turbulent wrinkled flame front with $\gamma^* < 1$.

An extinction or flame stretch factor $\mathcal{G}_{ext} \leq 1$ will be introduced in Section 1.7 to take into account flame quenching due to subgrid scales. This factor has effect on γ^* that is finally given by:

$$\gamma^* = \mathcal{G}_{ext}\,\frac{\mathcal{S}_\mathcal{T}}{\mathcal{S}_\mathcal{L}}\frac{\delta_\mathcal{F}}{\Delta}\,. \tag{1.2}$$

Reference	Reactants	Combustion Type	Pr Range
[12]	C_3H_8/Air	Premixed	0.70 – 0.74
[13]	CH_4/H_2/Air	Non-Premixed	0.48 – 0.74
[14]	$CO/H_2/N_2$/Air	Non-Premixed	0.45 – 0.71
[15]	$CO/H_2/N_2$/Air	Premixed	0.58 – 0.71

Tabella 1.1: Ranges of Prandtl number distributions obtained from numerical simulations of different flames.

The problem of γ^* estimation becomes the problem of estimating the characteristics of the local flame front in terms of its turbulent flame speed, laminar flame speed and thickness (turbulent or laminar) from the filtered conditions of the flow and depending on the related local premixed combustion regime.

The local filtered chemical time required to estimate laminar quantities can be calculated as $\tau_{ch} = \rho C_p T / |\Delta\mathcal{H}_R|$, where $\Delta\mathcal{H}_R = \sum_{i=1}^{N_s} \mathcal{H}_i \dot{\omega}_i$ is the heat of reaction, N_s being the number of chemical species, $\mathcal{H}_i = h^0_{f_i}(T_r) + \Delta h_{s_i}(T)$ the enthalpy of the $i-th$ chemical species, $h^0_{f_i}(T_r)$ its formation enthalpy at the reference temperature $T_r = 298.15\,\mathrm{K}$, $\Delta h_{s_i} = \int_{T_r}^{T} C_{p_i}(T)dT$ its sensible enthalpy, and $\dot{\omega}_i$ its reaction rate.

In the following, models to derive the turbulent quantities will be proposed.

1.2 Vortices / Flame Front Interaction

This Section addresses two issues related to the interaction between vortices and a flame front. The first deals with defining the range of scales that can interact with a flame front, and eventually enter into. This will be important to model local flame thickening due to turbulence. The second deals with defining the smallest turbulent scales that apply the highest strain rate and curvature wrinkling onto the flame front. This will be important to model local flame quenching due to turbulence.

1.2.1 The Smallest Surviving Eddy

The interaction between a premixed flame front and eddies has been widely analyzed in literature. Results clearly show that the dissipative Kolmogorov scales η cannot quench a flame front [11]. An estimate of the smallest turbulent scale that can affect a laminar flame front without being dissipated can be obtained by considering that the turbulent $l-$scale Damköhler number of second species has to be greater than one, i.e.,

$$Da_l^{II} = \frac{\tau_{\nu_l}}{\tau_{ch}} = Pr^{-1}\left(\frac{l}{\delta_{\mathcal{L}}}\right)^2 \geq 1\,, \tag{1.3}$$

where $\tau_{\nu_l} = l^2/\nu$ is the lifetime of the generic vortex of scale l, ν being the dynamic viscosity, $\tau_{ch} = \delta_{\mathcal{L}}/\mathcal{S}_{\mathcal{L}} = \delta^2_{\mathcal{L}}/\alpha$ is the chemical time, and $Pr = \nu/\alpha$ is the Prandtl number.

Similarly to the case $Re_l < 1$ for which eddies are destroyed by viscous dissipation before they can be convected and sustain the vortex cascade, so when $Da_l^{II} < 1$ eddies of scale l are destroyed by viscous dissipation before combustion can take place, as observed in [11]. From this point of view, Da_l^{II} is a measure of the generic vortex to penetrate a flame front. Furthermore, Da_l^{II} is also a good measure of curvature effects [11].

These considerations, confirmed by numerical simulations and experiments, lead to conclude that the η scales cannot quench a flame front. In fact, when $u'_l/S_L < 1$ interaction is weak, even though the η scales have $Da_l^{II} > 1$; when $l/\delta_L < 1$, $Da_l^{II} < 1$ and η scale fluctuations ($u'_l/S_L > 1$) are dissipated by viscous effects [11].

Hence, the smallest surviving scale l^* is estimated as

$$l^* = Pr^{1/2}\,\delta_{\mathcal{L}} = l_\Delta \left(Da^I_\Delta\, Re_\Delta\right)^{-1/2} = l_\Delta Da^{II^{-1/2}}_\Delta\,, \tag{1.4}$$

where $Re_\Delta = u'_\Delta l_\Delta/\nu$ is the turbulent Reynolds number defined in terms of the local length and velocity macroscales l_Δ and u'_Δ, $Da^I_\Delta = l_\Delta/\left(u'_\Delta \tau_{ch}\right)$ is the turbulent $l_\Delta-$scale Damköhler number of first species. Turbulent

scales larger than l^* will not be destroyed or damped by the flame front. It is observed that for $Pr = 1$, it is always $l^* \equiv \delta_{\mathcal{L}}$. Here, the $Pr = 1$ assumption is removed, in agreement with distributions of local Prandtl number obtained from numerical simulations of different flames, as shown in Table 1.1.

The smallest surviving scale $l^* \in [\eta, l_\Delta]$, and this is fulfilled for whatever Prandtl number if $l_\Delta \geq l^* \geq \eta \Leftrightarrow Re_\Delta^{-1} \leq Da_\Delta^I \leq Re_\Delta^{1/2}$, observing that $l^* = l_\Delta$ for $Da_\Delta^I = Re_\Delta^{-1}$ and $l^* = \eta$ for $Da_\Delta^I = Re_\Delta^{1/2}$.

An important observation is that $l^* \leq \delta_{\mathcal{L}} \Leftrightarrow Pr \leq 1$, and this means that in gaseous combustion ($Pr \leq 1$) eddy-scales smaller than the flame thickness may survive and affect the flame itself, e.g., entering into it (although this has not been proved yet) and thickening it.

1.2.2 The Smallest Wrinkling Eddy

Looking at vortices / flame front interaction problem, some eddies will be destroyed by viscous dissipation before combustion can take place. The range of the surviving eddy-scales has been defined in Section 1.2.1. Among these scales, those smaller than the local flame front thickness, may locally enter into it and thicken it provided that $u'_\Delta \geq \mathcal{S}_{\mathcal{L}}$, u'_Δ being the local *rms* velocity fluctuation. However, this "surviving" condition is not sufficient for an eddy to locally wrinkle a flame front. Only eddies with characteristic (tangential) velocity $u'_l \geq \mathcal{S}_{\mathcal{L}}$ will be able to locally wrinkle a flame front.

Hence, given the smallest surviving eddy $l^* = l_\Delta \left(Da_\Delta^I\, Re_\Delta\right)^{-1/2}$, the smallest surviving and wrinkling eddy l_w^* will be given by the condition

$$\frac{u'_{l^*}}{\mathcal{S}_{\mathcal{L}}} \geq 1 \Rightarrow \frac{u'_\Delta}{\mathcal{S}_{\mathcal{L}}}\left(\frac{l^*}{l_\Delta}\right)^{1/3} = Pr^{1/2}\left(Re_\Delta Da_\Delta^{I^{-2}}\right)^{1/3} \geq 1\,. \tag{1.5}$$

This means that the surviving scales l^* become l_w^*, i.e., able to locally wrinkle a flame front if $Da_\Delta^I \leq Pr^{3/4} Re_\Delta^{1/2}$. Substituting the maximum Damköhler number for the smallest surviving and wrinkling scale into Eqn. (1.4), the minimum surviving and wrinkling scale l_w^* is obtained, $l_w^*\big|_{min} = Pr^{-3/8}\,\eta \geq \eta$. Hence, it is observed that l_w^* decreases as $l_\Delta \left(Da_\Delta^I\, Re_\Delta\right)^{-1/2}$ by increasing Da_Δ^I up to $Da_\Delta^I = Pr^{3/4} Re_\Delta^{1/2}$. Then, l_w^* maintains its minimum value $Pr^{-3/8}\,\eta$ for whatever $Da_\Delta^I \geq Pr^{3/4} Re_\Delta^{1/2}$, implying that the highest local flame front curvature can be $2\, l_w^{*^{-1}} = 2\, Pr^{3/8}/\eta$.

From what found above, the minimum scale Reynolds number for flame front wrinkling will be

$$Re_{l_w^*}\big|_{min} = \frac{\mathcal{S}_{\mathcal{L}}\, l^*}{\nu} \equiv \frac{\mathcal{S}_{\mathcal{L}}\; l_w^*\big|_{min}}{\nu} = Pr^{-1/2} \geq 1\,. \tag{1.6}$$

It is observed that simple chemistry DNS calculations [11, 16] showed

$$\frac{l_w^*\big|_{min}}{\delta_{\mathcal{L}}} = 0.2 + 5.5\left(\frac{\varepsilon \delta_{\mathcal{L}}}{\mathcal{S}_{\mathcal{L}}{}^3}\right)^{-1/6} \Rightarrow Re_{l_w^*}\big|_{min} \approx 5.5^{3/2}\, Da_l^{I^{-1/2}}\, Pr^{-1}\,, \tag{1.7}$$

with $\varepsilon = u_l'^3/l$. Experimental work [17, 18] instead showed

$$\frac{u'_{l_w^*}\big|_{min}}{\mathcal{S}_{\mathcal{L}}} = 2.5\left(\frac{l_w^*\big|_{min}}{\delta_{\mathcal{L}}}\right)^{-1} \Rightarrow Re_{l_w^*}\big|_{min} \approx 2.5\, Pr^{-1}\,. \tag{1.8}$$

Large differences are expected between experiments, simple chemistry DNS calculations and theoretical results. However, the trends of these three different approaches are qualitatively well reproduced, looking at the $Re_{l_w^*}\big|_{min} = f\,(Pr)$ dependence.

1.3 Premixed Combustion Regimes

Thinking to the interaction between a flame front and turbulent eddies, it is possible to identify three main combustion regimes based on the comparison between the local laminar flame front $\delta_{\mathcal{L}}$, the local turbulent macroscale l_Δ, and the local turbulent dissipative scale η. These regimes are described in Table 1.2 and they are named

Regime	Scale Condition		Da^I_Δ Condition
$\mathcal{VR}$	$\delta_\mathcal{L} \geq l_\Delta$	$\Rightarrow$	$Da^I_\Delta \leq Pr^{-1}Re^{-1}_\Delta$
$\mathcal{TTC_R}$	$l_\Delta > \delta_\mathcal{L} \geq \eta$	$\Rightarrow$	$Pr^{-1}Re^{1/2}_\Delta \geq Da^I_\Delta > Pr^{-1}Re^{-1}_\Delta$
$\mathcal{WR}$	$\delta_\mathcal{L} < \eta$	$\Rightarrow$	$Da^I_\Delta > Pr^{-1}Re^{1/2}_\Delta$

Tabella 1.2: The three main premixed combustion regimes based on the comparison between turbulent length scales and laminar flame front thickness.

$\mathcal{VR}$ from $\mathcal{V}olumetric\,\mathcal{R}egime$, $\mathcal{TTC_R}$ from $\mathcal{T}hickened$, $\mathcal{T}urbulence-\mathcal{T}hickened$, $\mathcal{C}orrugated\,\mathcal{R}egimes$, $\mathcal{WR}$ from $\mathcal{W}rinkled\,\mathcal{R}egime$.

1.4 The $\mathcal{T}$urbulence-$\mathcal{T}$hickened $\mathcal{R}$egime: the Zimont Model

In Section 1.2.1 it was shown that some scales smaller than the flame thickness may not be dissipated. These scales may affect the flame front itself thickening it but leaving unchanged the chemical time: this is the base of Zimont's model [19, 20, 21]. According to this model the thickened flame front $\delta^*_\mathcal{F}$ can be estimated as

$$\delta^*_\mathcal{F} \approx l_\Delta Da^{I^{-3/2}}_\Delta \,, \tag{1.9}$$

and the turbulent tickened flame speed can be scaled as

$$\mathcal{S}_\mathcal{T}|_\mathcal{Z} \approx \mathcal{A}_\mathcal{Z} u'_\Delta Da^{I^{1/4}}_\Delta \,, \tag{1.10}$$

$\mathcal{A}_\mathcal{Z} = 0.5$ being an empirical constant [20, 22]. If the constant $\mathcal{A}_\mathcal{Z}$ is introduced in Eqn. (1.10), it has to be put also in Eqn. (1.9), i.e.,

$$\delta^*_\mathcal{F} \approx \mathcal{A}_\mathcal{Z} l_\Delta Da^{I^{-3/2}}_\Delta \,, \tag{1.11}$$

to keep the chemical time constant.

In terms of nondimensional Prandtl and turbulent Reynolds numbers, $\mathcal{S}_\mathcal{T}/\mathcal{S}_\mathcal{L}|_\mathcal{Z}$ becomes

$$\left.\frac{\mathcal{S}_\mathcal{T}}{\mathcal{S}_\mathcal{L}}\right|_\mathcal{Z} \approx \mathcal{A}_\mathcal{Z} \left(PrRe_\Delta\right)^{1/2} Da^{I^{-1/4}}_\Delta \,. \tag{1.12}$$

Assuming the chemical time unchanged, the thickness of the turbulent flame front is

$$\left.\delta^\mathcal{T}_\mathcal{F}\right|_\mathcal{Z} \approx \mathcal{S}_\mathcal{T}|_\mathcal{Z}\, \tau_{ch} \approx \mathcal{A}_\mathcal{Z} l_\Delta Da^{I^{-3/4}}_\Delta \,, \tag{1.13}$$

so that $\delta^\mathcal{T}_\mathcal{F}/\ \mathcal{S}_\mathcal{T}|_\mathcal{Z} = \tau_{ch}$.

Imposing the conditions reported in Table 1.3, the $\mathcal{T}urbulence$ - $\mathcal{T}hickened$ flame $\mathcal{R}egime$ validity ranges are obtained in terms of the local Damköhler number, Da^I_Δ. The range for gaseous combustion characterized by $Pr < 1$, here named $\mathcal{Z}2$ regime, is reported in Table 1.4.

Condition 8 in Table 1.3 is here justified. The expression for the local reacting volume fraction γ^*, Eqn. (1.2), in the turbulent thickened flame regime becomes:

$$\gamma^* = \mathcal{G}_{ext}\,\frac{\mathcal{S}_\mathcal{T}}{\mathcal{S}_\mathcal{L}}\frac{\delta_\mathcal{F}}{\Delta} = \mathcal{G}_{ext}\,\left.\frac{\mathcal{S}_\mathcal{T}}{\mathcal{S}_\mathcal{L}}\right|_\mathcal{Z}\frac{\delta^*_\mathcal{F}}{\Delta} \,, \tag{1.14}$$

with $\mathcal{S}_\mathcal{T}/\mathcal{S}_\mathcal{L}|_\mathcal{Z}$ and $\delta^*_\mathcal{F}$ given by Eqns. (1.10) and (1.11). Without considering the effect of $\mathcal{G}_{ext}$, i.e., assuming $\mathcal{G}_{ext} = 1$ in Eqn. (1.14), the volume fraction γ^* has to be less than one.

List	Condition	Type of Condition		Range
1	$\delta_{\mathcal{L}} \leq l_{\Delta}$	subgrid modelling 1	$\Rightarrow$	$Da^I_{\Delta} \geq Pr^{-1} Re^{-1}_{\Delta}$
2	$\delta_{\mathcal{L}} \geq \eta$	minimum thickening	$\Rightarrow$	$Da^I_{\Delta} \leq Pr^{-1} Re^{1/2}_{\Delta}$
3	$\delta^*_{\mathcal{F}} \geq \delta_{\mathcal{F}}$	thickening effect 1	$\Rightarrow$	$Da^I_{\Delta} \leq Pr^{1/2} Re^{1/2}_{\Delta}$
4	$\delta^{\mathcal{T}}_{\mathcal{F}} \geq \delta^*_{\mathcal{F}}$	thickening effect 2	$\Rightarrow$	$Da^I_{\Delta} \geq 1$
5	$\delta^{\mathcal{T}}_{\mathcal{F}} \leq l_{\Delta}$	subgrid modelling 2	$\Rightarrow$	$Da^I_{\Delta} \geq 1$
6	$l^*_{tk} \geq l^*$	minimum scale	$\Rightarrow$	$Da^I_{\Delta} \leq Re^{1/2}_{\Delta}$
7	$u'_{\Delta} \geq \mathcal{S}_{\mathcal{L}}$	velocity fluctuation	$\Rightarrow$	$Da^I_{\Delta} \leq Pr^{-1} Re_{\Delta}$
8	$\frac{\mathcal{S}_{\mathcal{T}}}{\mathcal{S}_{\mathcal{L}}} \frac{\delta^*_{\mathcal{F}}}{\Delta} \leq 1$	reacting volume fraction	$\Rightarrow$	$Da^I_{\Delta} \geq Pr^{2/7} Re^{2/7}_{\Delta}$

Tabella 1.3: Conditions applied to determine the validity range of the $\mathcal{T}urbulence$-$\mathcal{T}hickened$ flame $\mathcal{R}egime$.

Range	Pr Condition		Da^I_{Δ} Condition
$\mathcal{Z}2_N$	$1 \geq Pr \geq Re^{-1}_{\Delta}$	$\Rightarrow$	$Pr^{1/2} Re^{1/2}_{\Delta} \geq Da^I_{\Delta} \geq Pr^{2/7} Re^{2/7}_{\Delta}$

Tabella 1.4: Validity range of the $\mathcal{T}urbulence$-$\mathcal{T}hickened$ flame $\mathcal{R}egime$ for gaseous combustion characterized by $Pr \leq 1$.

1.5 A Closer Look to Premixed Combustion Regimes

The premixed combustion regimes described in Section 1.3 are here analysed in more details considering the model developed in Section 1.4. In particular, depending on the local Prandtl number, there can be four possible conditions. The most likely to happen condition in gaseous combustion (also in supercritical condition) is $1 \geq Pr \geq Re^{-1}_{\Delta}$. The ranges of combustion regimes associated to this condition are shown in Table 1.5.

Hence, $1 \geq Pr \geq Re^{-1}_{\Delta}$ is the sole condition that will be considered in detail and used to develop a subgrid turbulent combustion closure for the chemical source rate. This assumption implies that the subgrid scale model for turbulence / combustion interaction would be switched on for $Re_{\Delta} \geq Pr^{-1}$, being $Pr \leq 1$ ($Re_{\Delta} \geq 1.35$ and 2.22 at $Pr = 0.74$ and 0.45, respectively, considering the extreme values in Table 1.1). For $Re_{\Delta} < Pr^{-1}$ the subgrid flame would be considered locally laminar. However, another assumption will be here taken, furtherly increasing the activation cell Reynolds number.

Considering the smallest surviving and wrinkling scale l^*_w defined in Section 1.2.2, it is observed that the minimum scale Reynolds number for flame front wrinkling is $Re_{l^*_w}\big|_{min} = Pr^{-1/2}$, as shown in Eqn. (1.6). Hence, this will be also the minimum computational cell Reynolds number to switch the subgrid turbulent combustion model on (this is guaranteed since the model is activated at least for $Re_{\Delta} \geq Pr^{-1}$. At $Da^I_{\Delta}\big|_{l^*_{w,min}} = Pr^{3/4} Re^{1/2}_{\Delta}$, the scale l^*_w reaches its minimum value $Pr^{-3/8}\,\eta$, then maintained for whatever $Da^I_{\Delta} \geq Pr^{3/4} Re^{1/2}_{\Delta}$. For $1 \geq Pr \geq Re^{-1}_{\Delta}$ this particular Da^I_{Δ} is located as: $(PrRe_{\Delta})^{1/2} \geq Da^I_{\Delta}\big|_{l^*_{w,min}} \geq (PrRe_{\Delta})^{2/7}$ for $1 \geq Pr \geq Re^{-6/13}_{\Delta}$, and $(PrRe_{\Delta})^{2/7} > Da^I_{\Delta}\big|_{l^*_{w,min}} > 1$ for $Re^{-6/13}_{\Delta} > Pr \geq Re^{-1}_{\Delta}$. Note that for $Pr = Re^{-6/13}_{\Delta}$, it is $Da^I_{\Delta}\big|_{l^*_{w,min}} \equiv (PrRe_{\Delta})^{2/7}$, i.e., it is located at the lower boundary of the $\mathcal{T}urbulence$-$\mathcal{T}hickened$ $\mathcal{R}egime$.

In order to have a sufficiently high minimum cell Reynolds number to guarantee a minimum subgrid turbulence / combustion interaction, it is here assumed to increase the activation cell Reynolds number by considering only the range $1 \geq Pr \geq Re^{-6/13}_{\Delta}$ for the subgrid scale turbulent combustion model. This assumption implies that the subgrid scale model for turbulence / combustion interaction will be switched on for $Re_{\Delta} \geq Pr^{-13/6}$, being $Pr \leq 1$ ($Re_{\Delta} \geq 1.92$ and 5.64 at $Pr = 0.74$ and 0.45, respectively, considering the extreme values in Table 1.1). For $Re_{\Delta} < Pr^{-13/6}$ the subgrid flame will be considered locally laminar.

Details about the selected group of turbulent combustion regimes with the validity range $1 \geq Pr \geq Re^{-6/13}_{\Delta}$ are provided in Fig. 1.1. It is observed that all the information in this figure are also valid for $1 \geq Pr \geq Re^{-1}_{\Delta}$, apart from the location of the $Da^I_{\Delta}\big|_{l^*_{w,min}}$. In particular, this figure shows the ranges of the combustion regimes

$1 \geq Pr \geq Re_\Delta^{-1}$		
$\mathcal{V}_\mathcal{R}$	$\mathcal{TTC}_\mathcal{R}$	$\mathcal{W}_\mathcal{R}$
$Da_\Delta^I \leq (PrRe_\Delta)^{-1} (\leq 1)$	$Pr^{-1}Re_\Delta^{1/2} \geq Da_\Delta^I \geq (PrRe_\Delta)^{-1}$	$Da_\Delta^I \geq Pr^{-1}Re_\Delta^{1/2}$
	$\mathcal{Z}2_N \subset \mathcal{TTC}_\mathcal{R}$	
	$(PrRe_\Delta)^{1/2} \geq Da_\Delta^I \geq (PrRe_\Delta)^{2/7}$	

Tabella 1.5: Ranges of the premixed turbulent combustion regimes when $1 \geq Pr \geq Re_\Delta^{-1}$, that is the most likely to happen condition in gaseous combustion (also in supercritical condition).

and the ordered list of the main scales of turbulence and combustion. Specific values of some scales are also highlighted. In the same figure, it is also evidenced that if $Pr = 1$ or $Pr = Re_\Delta^{-1}$, some regimes collapse. In particular, if $Pr = 1$ the *Corrugated Regime* disappears, and in the *Volumetric Regime* it is always $l^* > l_\Delta$. If $Pr = Re_\Delta^{-1}$ the *Thickened* and *Turbulence-Thickened Regimes* disappear (however, this can not happen due to the limiting assumption $1 \geq Pr \geq Re_\Delta^{-6/13}$).

1.6 Modelling the Reacting Volume Fraction

The reacting volume fraction γ^* in Eqn. (1.1) will have to be modelled differently depending on the combustion regimes shown in Fig. 1.1. In this Section the effect of quenching due to turbulent scales, i.e., the $\mathcal{G}_{ext}$ function, is not taken into account. Hence, attention is posed on

$$\gamma^* = \frac{\mathcal{S}_\mathcal{T}}{\mathcal{S}_\mathcal{L}} \frac{\delta_\mathcal{F}}{\Delta} . \tag{1.15}$$

For subgrid turbulent combustion, i.e., $Re_\Delta \geq Pr^{-13/6}$, with $Pr \leq 1$, γ^* is modelled as

- *Volumetric Regime*

$$\gamma^* = 1 \tag{1.16}$$

- *Thickened Regime*

$$\gamma^* = \frac{\delta_\mathcal{L}}{\Delta} = \left(Pr\, Re_\Delta\, Da_\Delta^I\right)^{-1/2} \leq 1 \tag{1.17}$$
$$\gamma^*\big|_{max} = 1 \qquad \gamma^*\big|_{min} = (Pr\, Re_\Delta)^{-9/14} \leq 1$$

- *Turbulence-Thickened Regime*

$$\gamma^* = \frac{\mathcal{S}_\mathcal{T}}{\mathcal{S}_\mathcal{L}}\bigg|_\mathcal{Z} \frac{\delta_\mathcal{F}^*}{\Delta} = \mathcal{A}_\mathcal{Z} \left(Pr\, Re_\Delta\, Da_\Delta^{I^{-7/2}}\right)^{1/2} < 1 \tag{1.18}$$
$$\gamma^*\big|_{max} = \mathcal{A}_\mathcal{Z} < 1 \qquad \gamma^*\big|_{min} = \mathcal{A}_\mathcal{Z}\, (Pr\, Re_\Delta)^{-3/8} < 1$$

- *Corrugated Regime*

$$\gamma^* = \frac{\mathcal{S}_\mathcal{T}}{\mathcal{S}_\mathcal{L}}\bigg|_\mathcal{C} \frac{\delta_\mathcal{L}}{\Delta} \approx \frac{\mathcal{S}_\mathcal{T}}{\mathcal{S}_\mathcal{L}}\bigg|_\mathcal{Z} \frac{\delta_\mathcal{L}}{\Delta} = \mathcal{A}_\mathcal{Z} Da_\Delta^{I^{-3/4}} < 1 \tag{1.19}$$
$$\gamma^*\big|_{max} = \mathcal{A}_\mathcal{Z}\, (Pr\, Re_\Delta)^{-3/8} < 1 \qquad \gamma^*\big|_{min} = \mathcal{A}_\mathcal{Z} \left(Pr^{-2}\, Re_\Delta\right)^{-3/8} < 1$$

  having used the Zimont expression for $\mathcal{S}_\mathcal{T}$ also in this regime due to the lack of reliable experimental data [22] and the superiority of Zimont model with respect to other models [22];

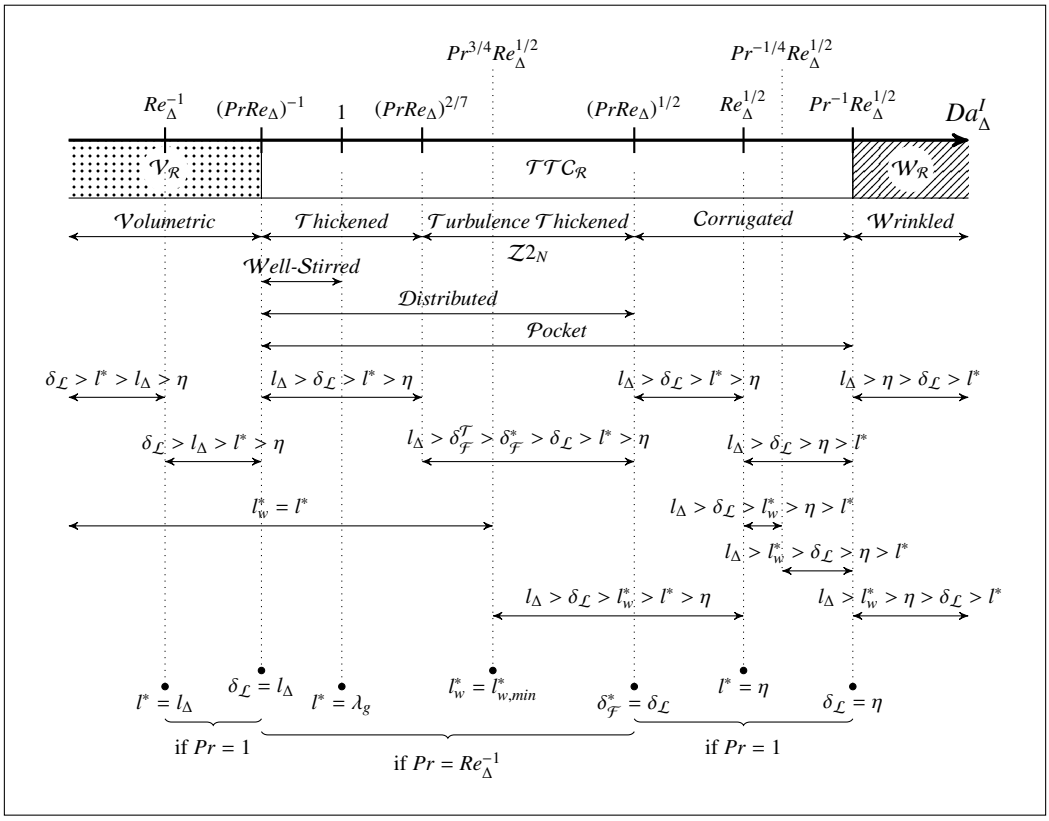

Figura 1.1: Description of the turbulent combustion regimes for $1 \geq Pr \geq Re_\Delta^{-6/13}$, i.e., for $Re_\Delta \geq Pr^{-13/6}$, with $Pr \leq 1$. Main scales of turbulence and combustion are also compared and ordered. Note that information in this figure are also valid for $1 \geq Pr \geq Re_\Delta^{-1}$, apart from the location of $Da_\Delta^I\big|_{l_{w,min}^*} = Pr^{3/4}Re_\Delta^{1/2}$ that would be located between 1 and $(PrRe_\Delta)^{2/7}$ for $Re_\Delta^{-6/13} > Pr \geq Re_\Delta^{-1}$.

- *Wrinkled Regime*

$$\gamma^* = \frac{\mathcal{S}_\mathcal{T}}{\mathcal{S}_\mathcal{L}}\bigg|_\mathcal{W} \frac{\delta_\mathcal{L}}{\Delta} \approx \frac{\delta_\mathcal{L}}{\Delta} = \left(Pr\, Re_\Delta\, Da_\Delta^I\right)^{-1/2} \leq 1 \tag{1.20}$$
$$\gamma^*\big|_{max} = Re_\Delta^{-3/4} = \frac{\eta}{l_\Delta} \leq 1 \qquad \gamma^*\big|_{min} \to 0$$

  having neglected, for the time being, subgrid hydrodynamic effects and Lewis number effects on $\mathcal{S}_\mathcal{T}$. However, it is observed that this regime appears to be of minor importance to industrial applications [22]. Work is currently going on by the present authors to define, in this low strain regime (Markstein regime), a $\mathcal{X}$ factor taking into account thermo-diffusive effects (induced by reactants' Lewis number) that increase or decrease the turbulent flame speed and flame wrinkling: $\mathcal{S}_\mathcal{T}/\mathcal{S}_\mathcal{L} = 1 - \mathcal{X}$, with $\mathcal{X} > 0$ or $\mathcal{X} < 0$ depending on local curvature, strain and Markstein number signs.

It is observed that $\Delta \equiv l_\Delta$ was assumed in deriving the non-dimensional number dependence in previous expressions, and that all of them guarantee $\gamma^* \leq 1$.

For subgrid laminar or pseudo-laminar combustion, i.e., $Re_\Delta < Pr^{-13/6}$, γ^* is modelled as

- *Laminar Volumetric Regime* ($\delta_\mathcal{L} \geq \Delta$)

$$\gamma^* = 1 \tag{1.21}$$

- *Laminar* (Planar) *Flamelet Regime* ($\delta_\mathcal{L} < \Delta$)

$$\gamma^* = \frac{\delta_\mathcal{L}}{\Delta} < 1\,. \tag{1.22}$$

1.7 The Extinction Factor

Turbulent eddies can stretch a flame front up to local quenching. Hence, considering this effect in modeling turbulent premixed flames is mandatory. In literature there are already some models for quenching. Here, a couple of them are highlighted and one chosen to estimate the extinction or stretch factor $\mathcal{G}_{ext} \leq 1$ in Eqn. (1.2).

It is observed that when $\mathcal{G}_{ext} = 1$ at subgrid level does not imply that stretching is not experienced by the flame at all. It means that the subgrid turbulence is so weak not to effectively stretch the subgrid flamelets, but the resolved velocity fluctuations may be high enough to effectively stretch the resolved flame front.

A model that can be easily used to predict quenching is the so called *quenching cascade model* [23], that compares quite well with experimental and direct numerical simulation data on quenching [18, p. 212-214]. The extinction region predicted by the *quenching cascade model* has been validated with experimental data [11, 18, 23]: high velocity fluctuations are required to produce localized flame quenching.

2 Validation of the Suggested Model

The Localised Turbulent Scale Model (LTSM) was developed in the previous year. Simulations of some test cases numerically defined and investigated by means of Direct Numerical Simulation by different authors, confirmed that several combustion regimes may be experienced in flames, as predicted by the model. Since the present authors came across some difficulties in obtaining the data of the DNSs selected in the previous year to validate the LES data and LTSM model, the present authors decided to define a new numerical test case. This new test case deals with premixed combustion of hydrogen enriched natural gas (HENG) and represents an important database at international level.

2.1 The HENG DNS Test Case

The Localised Turbulent Scale Model has been validated by simulating a test case defined and simulated by these authors using the Direct Numerical Simulation approach. In particular, the time average and rms fluctuation of some quantities resulted from the LES simulation were compared with their DNS counterpart.

The test case consists in an unconfined and athmospheric Bunsen flame developing along the streamwise diirection (z), as shown in Fig. 2.1. This premixed flame is produced by three adjacent rectangular slot burners whose size is undefined in the spanwise direction (x) and that are separated along the transversal direction (y) by means of two 0.17 mm thick walls. The central slot burner injects a fresh mixture of methane, hydrogen and air, while the two side burners inject hot combustion products of the same central mixture. This test case was selected because a slot Bunsen flame represents one of the major categories of turbulent premixed combustion. It is also interesting to analyse the effect of hydrogen added to methane, due to the increasing interest in hydrogen enriched natural gas.

The reactant mixture, with an equivalence ratio $\Phi = 0.7$ and with 0.2 mole fraction of hydrogen, is injected from the central slot with a bulk velocity of $100\,\mathrm{m\,s^{-1}}$ and at 600 K. The velocity of the coflow stream is $25\,\mathrm{m\,s^{-1}}$. The central jet Reynolds number is 2264, based on the width of the jet, 1.2 mm, its bulk velocity, and the kinematic viscosity $5.3 \cdot 10^{-5}\,\mathrm{m^2\,s^{-1}}$. Homogeneous isotropic turbulence is forced at the inlet. Such turbulence is artificially produced by means of a synthetic turbulence generator implemented from [24]. In particular, the spatial correlation length scales and velocity fluctuations provided as input to this generator are: $L_{zz} = 0.8\,\mathrm{mm}$, $L_{xx} = L_{yy} = L_{zz}/2 = 0.4\,\mathrm{mm}$, $u'_z = u'_x = u'_y = 12\,\mathrm{m\,s^{-1}}$ with no shear stresses (the Reynolds stress tensor is diagonal) [25].

The actual velocity fluctuation at the end of the injection channel is $u' \approx 12\,\mathrm{m\,s^{-1}}$, and the turbulent length scale is $l_t \approx 1$ mm. These data are used in the calculation of the characteristic numbers associated to the present jet premixed flame.

The central jet turbulent Reynolds number is 226, based on the rms velocity fluctuation, $12\,\mathrm{m\,s^{-1}}$, the integral scale, 1 mm, and the previous kinematic viscosity. The Kolmogorov length scale is $\eta \approx 17.22\,\mu$m. The adiabatic flame temperature is 2071 K. The laminar flame speed and flame front thickness at these conditions are $\mathcal{S}_\mathcal{L} = 0.96\,\mathrm{m\,s^{-1}}$ and $\delta_\mathcal{F} = 0.386$ mm, respectively. Hence, $u'_{rms}/\mathcal{S}_\mathcal{L} = 12.5$ and $L_t/\delta_\mathcal{F} = 2.6$; $Ka_\eta = 503$, $Da^I_{L_t} = 0.21$, thus locating this flame into the broken reaction regime of the standard combustion diagram, where turbulence is expected to strongly influence premixed flame structures.

This test was performed on a three-dimensional computational domain with 61 nodes in the spanwise direction (x), extending from -1.5 to 1.5 mm, and along which periodic boundary conditions are forced. The computational domain has four zones: a central injection zone extending from -4 mm to 0 in the streamwise direction (z) with a width (along y) of 1.2 mm and with 60×35 nodes (zy); two surrounding zones extending

from −0.4 mm to 0 in the streamwise direction and from the central slot external wall (wall thickness 0.17 mm) up to 18 mm outward in the transversal direction (y) with 8×89 nodes (zy); a main mixing and reacting zone downstream of the injection extending from 0 to 24 mm in the streamwise direction and from −18 mm to 18 mm in the transversal direction with 241×221 nodes (zy). The whole computational domain has 56785×61 = 3463885 nodes.

Seventeen species are transported: CH_4, H_2, O_2, N_2, OH, O, H, HO_2, H_2O_2, CH_3, CH_2, CH, CH_2O, HCO, CO, CO_2, H_2O. The chemical mechanism adopted for combustion is a skeletal mechanism having 58 reactions [26]. The walls are assumed viscous and adiabatic. Partially non-reflecting outflow boundary conditions were imposed at the open boundaries of the computational domain. The subgrid scale model adopted for the turbulence closure is the dynamic Smagorinsky model.

Temperature, streamwise and transversal velocities predicted through the LES simulation are compared with DNS data, in terms of their time averages and rms fluctuations transversal profiles at different heights above injection (see Figs. 2.2-2.4). Mass fractions are compared in terms of their time averages at the same locations (see Fig. 2.5). It is observed that the H_2O profiles are not reported since they are very similar to the CO_2 profiles, both in shape and value. The agreement between LES data obtained by using the LTSM model and the DNS data is very good, hence demonstrating the goodness of the new subgrid model.

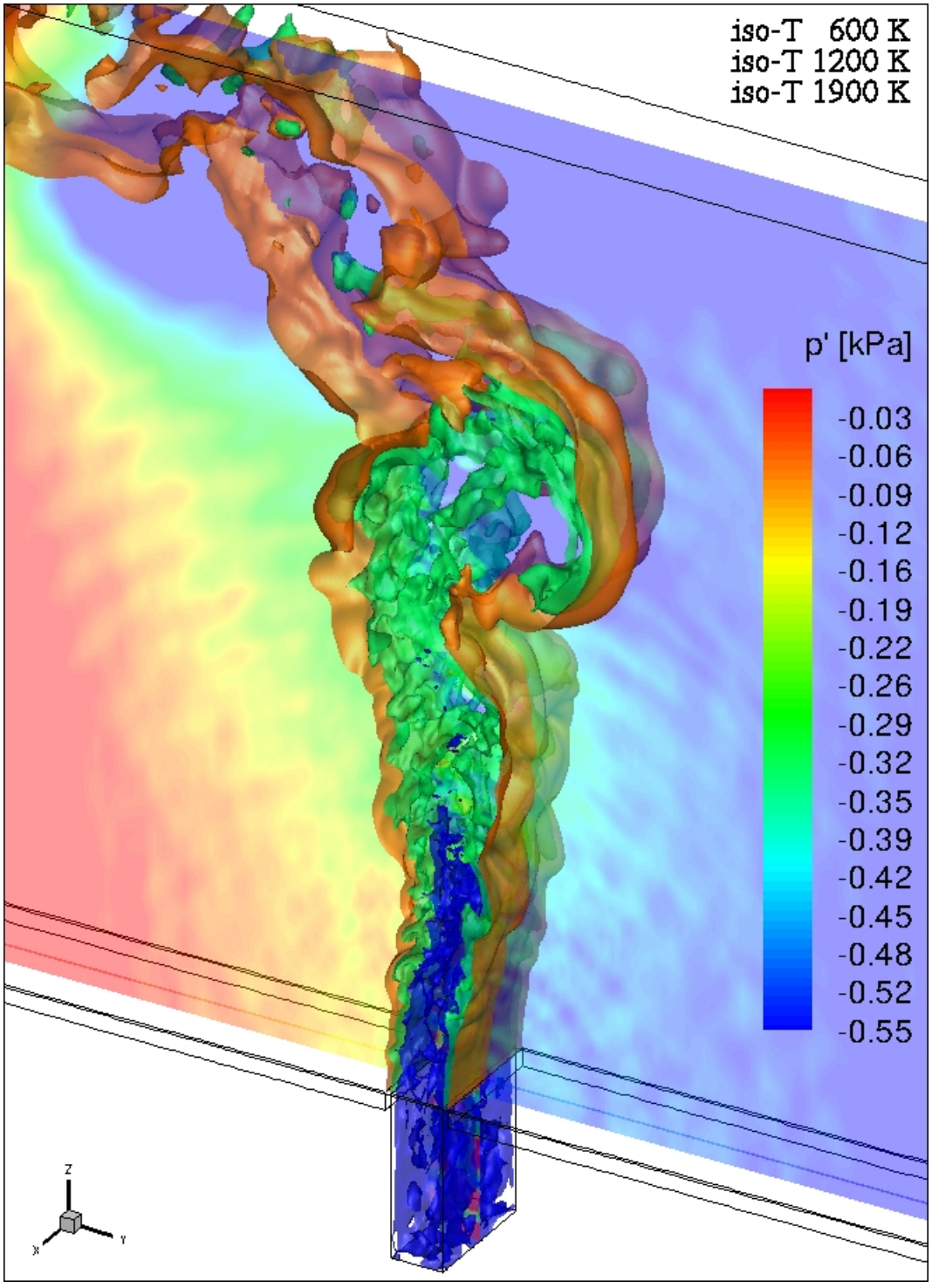

Figura 2.1: Instantaneous temperature iso-surfaces and pressure fluctuations in the middle plane.

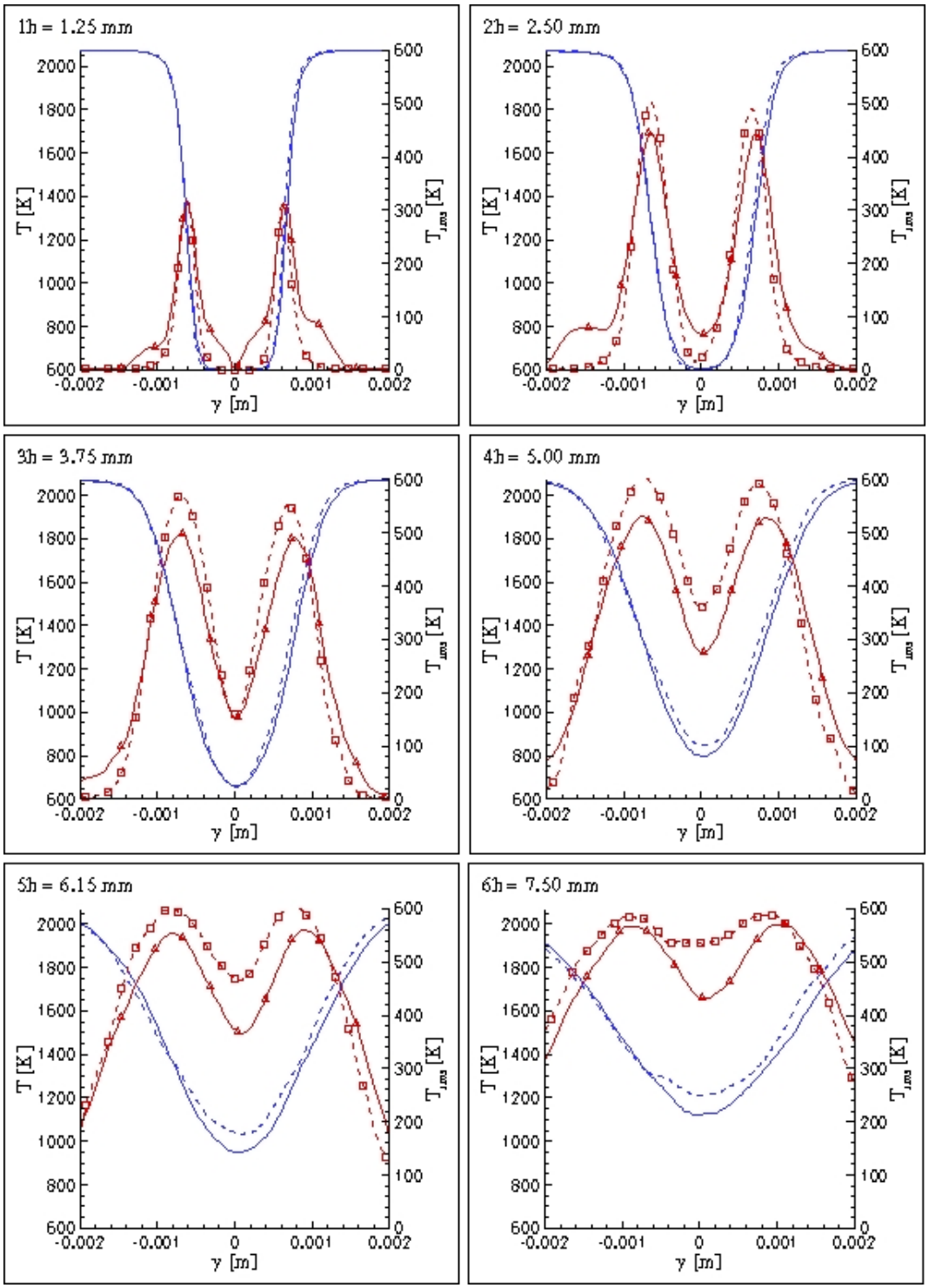

Figura 2.2: Transversal average and rms temperature profiles at several heights above injection: comparison between LES (solid lines) and DNS data (dashed lines). Lines with symbols are rms fluctuations.

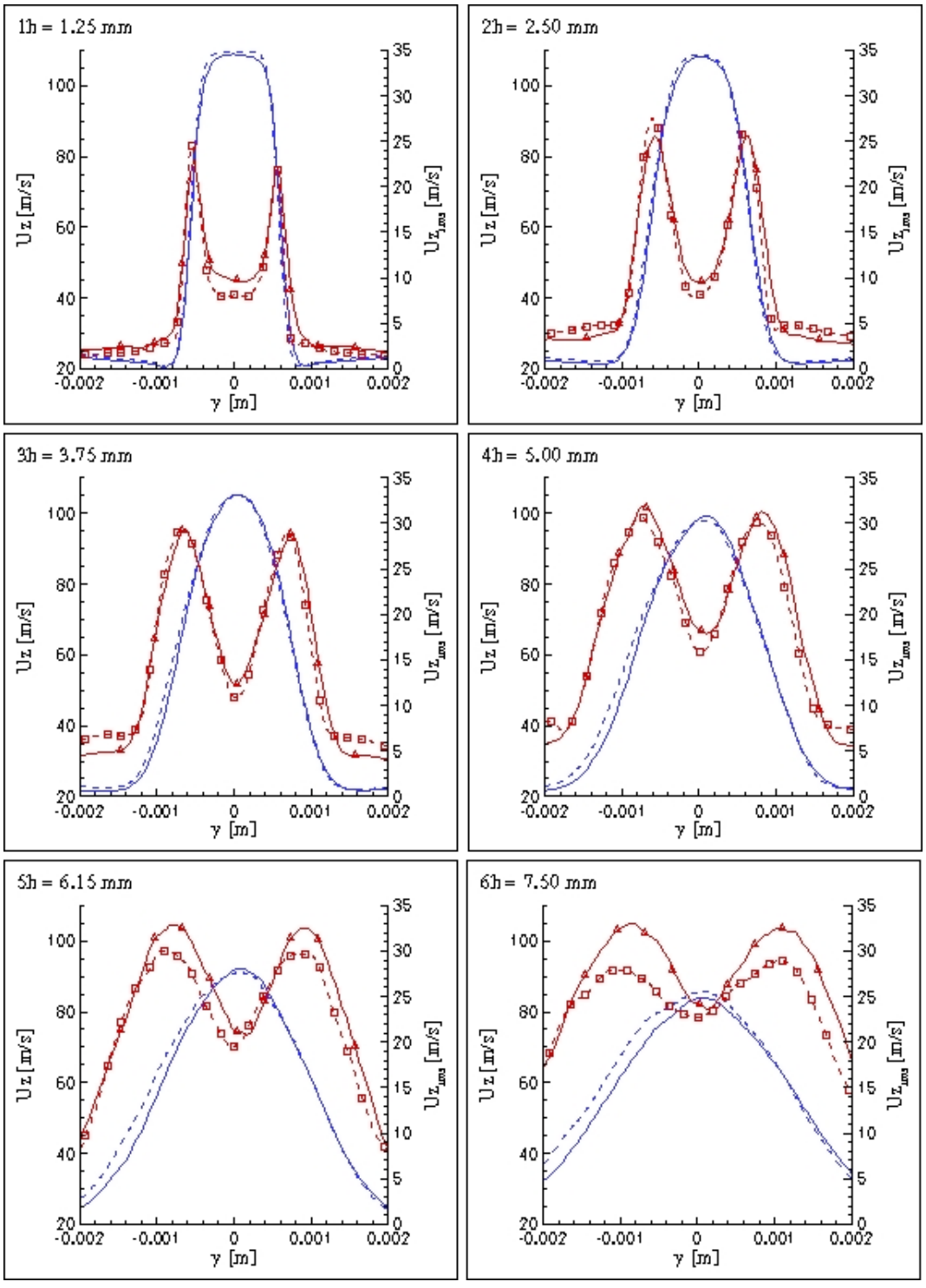

Figura 2.3: Transversal average and rms streamwise velocity profiles at several heights above injection: comparison between LES (solid lines) and DNS data (dashed lines). Lines with symbols are rms fluctuations.

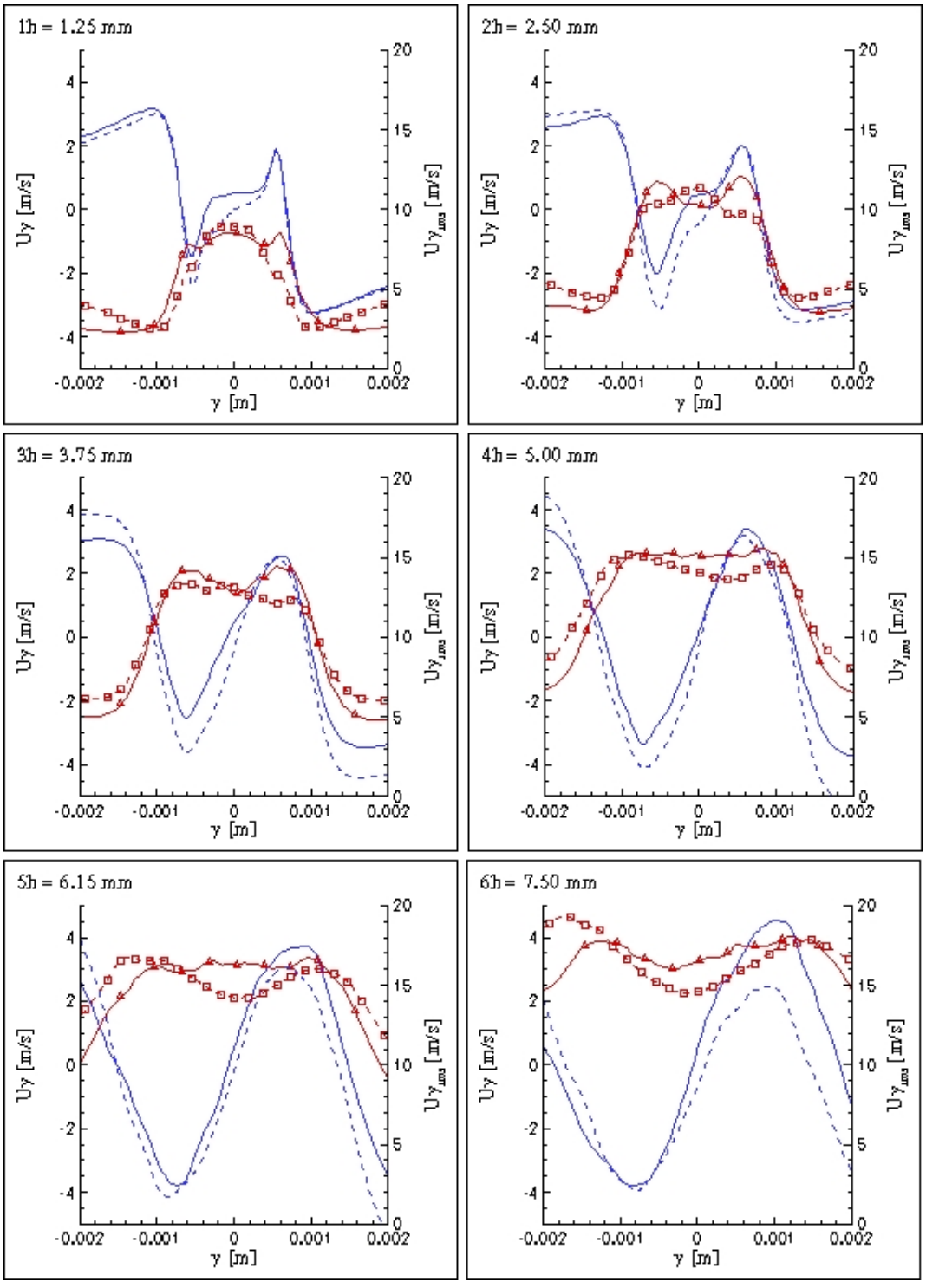

Figura 2.4: Transversal average and rms transversal velocity profiles at several heights above injection: comparison between LES (solid lines) and DNS data (dashed lines). Lines with symbols are rms fluctuations.

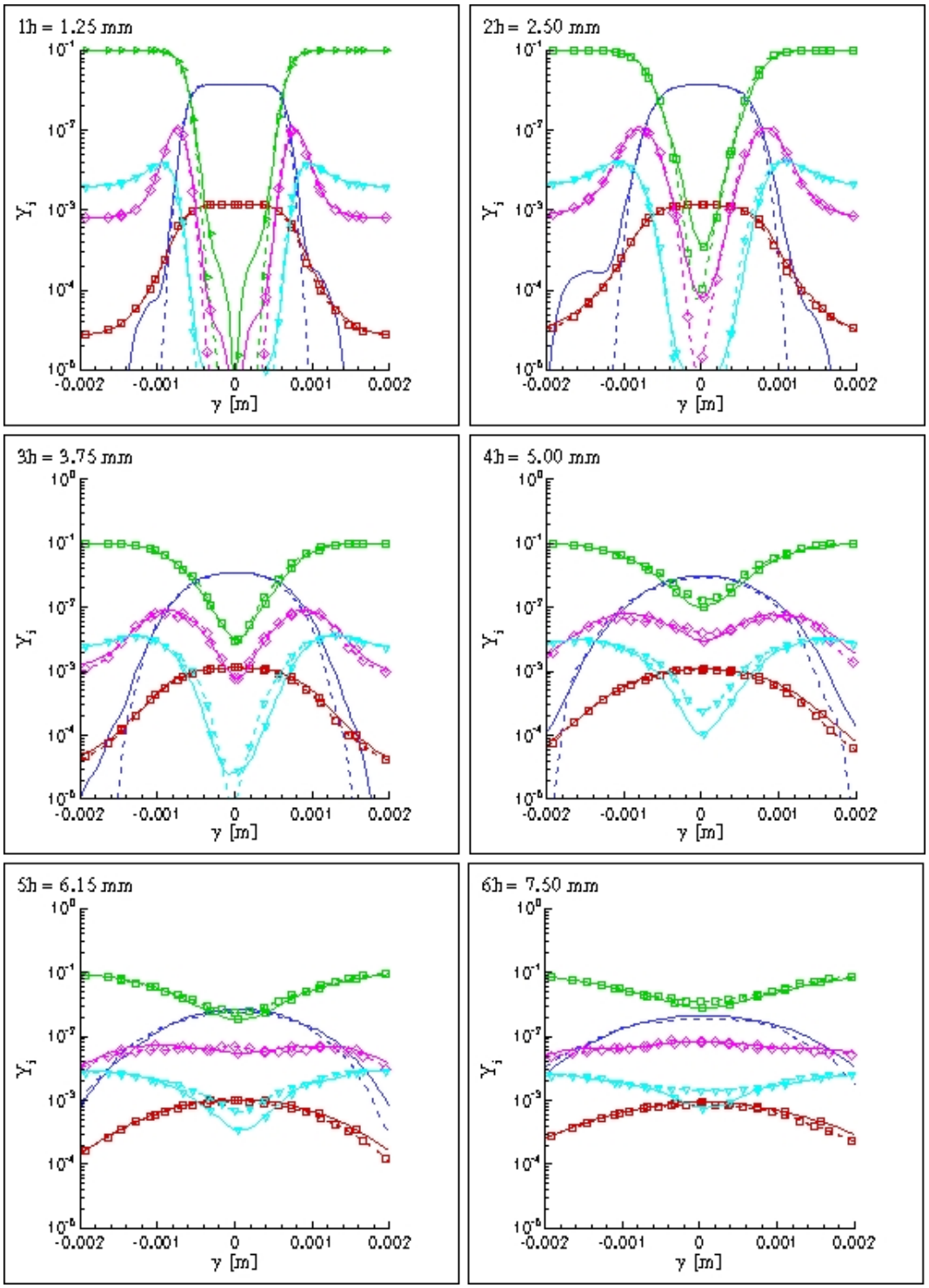

Figura 2.5: Transversal average mass fraction profiles at several heights above injection: comparison between LES (solid lines) and DNS data (dashed lines): no symbol, CH_4; $\triangle$, H_2; $\triangleright$, CO_2; $\diamond$, CO; $\triangledown$, OH.

Bibliografia

[1] Williams F.A. *Combustion Theory*. Addison-Wesley Publishing Company, 2nd edition, 1985.

[2] Barrere M. Modeles de combustion. *Revue Gen. Thermique*, 148:295, 1974.

[3] Bray K.N.C. Turbulent flows with premixed reactants in turbulent reacting flows. In Libby P.A. and Williams F.A., editors, *Topics in Applied Physics*, volume 44, page 115. Springer, 1980.

[4] Borghi R. On the structure and morphology of turbulent premixed flames. In Bruno C. and Casci C., editors, *Recent Advances in Aerospace Science*, page 117. Plenum, 1985.

[5] Borghi R. Turbulent combustion modelling. *Progress in Energy and Combustion Science*, 14:245–292, 1988.

[6] Peters N. Laminar flamelet concepts in turbulent combustion. In *Twenty First Symposium (International) on Combustion*, page 1231, Pittsburg, 1986. The Combustion Institute.

[7] Abdel-Gayed R.G. and Bradley D. Criteria for turbulent propagation limits of premixed flames. *Combustion and Flame*, 62:61, 1985.

[8] Abdel-Gayed R.G. and Bradley D. Combustion regimes and the straining of turbulent premixed flames. *Combustion and Flame*, 76:213, 1989.

[9] Chomiak J. *Combustion: A study in Theory, Fact and Application*. Abacus Press / Gordon and Breach Science Publishers, New York, 1990.

[10] Domingo P., Vervisch L., Payet S., and Hauguel R. DNA of a premixed turbulent V flame and LES of a ducted flame using a FSD-PDF subgrid scale closure with FPI-tabulated chemistry. *Combustion and Flame*, 143:566–586, 2005.

[11] Poinsot T., Veynante D., and Candel S. Quenching processes and premixed turbulent combustion diagrams. *Journal of Fluid Mechanics*, 228:561–606, 1991.

[12] Giacomazzi E., Battaglia V., and Bruno C. The coupling of turbulence and chemistry in a premixed bluff-body flame as studied by LES. *Combustion and Flame*, 138(4):320–335, 2004.

[13] Giacomazzi E., Favini B., Bruno C., Picchia F.R., and Arcidiacono N. LES of H2/CH4/Air turbulent non-premixed flame. In *European Combustion Meeting*, 25-28 October 2003. Orleans, France.

[14] Giacomazzi E., Picchia F.R., Arcidiacono N., Cecere D., Donato F., and Favini B. Unsteady simulation of a CO/H2/N2/Air turbulent non-premixed flame. *Combustion Theory and Modeling*, 12(6):1125–1152, 2008.

[15] Giacomazzi E., Cecere D., Donato F., Picchia F.R., Arcidiacono N., Daniele S., and Jansohn P. LES analysis of a syngas turbulent premixed dump-combustor at 5 bar. In *XXXIII Event of the Italian Section of the Combustion Institute and II S4FE*, http://www.combustioninstitute.it, 17-20 June 2010. Ischia, Italy.

[16] Gulder O.L. and Smallwood G.J. Inner cutoff scale of flame surface wrinkling in turbulent premixed flames. *Combustion and Flame*, 103:107–114, 1995.

[17] Roberts W.L., Driscoll J.F., Drake M.C., and Goss L.P. Images of the quenching of a flame by a vortex: to quantify regimes of turbulent combustion. *Combustion and Flame*, 94:58–69, 1993.

[18] Poinsot T. and Veynante D. *Theoretical and Numerical Combustion*. Edwards, Philadelphia, 2nd edition, 2005.

[19] Zimont VL. The theory of turbulent combustion at high reynolds numbers. *Combustion Explosions and Shock Waves*, 15:305–311, 1979.

[20] Zimont VL.and and Lipatnikov A.N. A numerical model of premixed turbulent combustion of gases. *Chem. Phys. Reports*, 14(7):993–1025, 1995.

[21] Zimont VL.and Biagioli F. and Syed K. Modelling turbulent premixed combustion in the intermediate steady propagation regime. *Progress in Computational Fluid Dynamics*, 1(1-3):14–28, 2001.

[22] Lipatnikov A.N. and Chomiak J. Turbulent flame speed and thickness: Phenomenology, evaluation, and apllication in multi-dimensional simulations. *Progress in Energy and Combustion Science*, 28:1–74, 2002.

[23] Meneveau C. and Poinsot T. Stretching and quenching of flamelets in premixed turbulent combustion. *Combustion and Flame*, 86:311–332, 1991.

[24] Klein M., Sadiki A., and Janicka J. A digital filter based generation of inflow data for spatially developing direct numerical or large eddy simulations. *J. of Computational Physics*, 186:652–665, 2003.

[25] Gence J.N. Homogeneous turbulence. *Annual Review in Fluid Mechanics*, 15:201–222, 1983.

[26] Smooke M.D., Puri I.K., and Seshadri K. A comparison between numerical calculations and experimental measurements of the structure of a counterflow diffusion flame burning diluted methane in diluted air. In *Proceedings of the 22nd Symposium International on Combustion, The Combustion Institute*, volume 21, pages pp. 1783–1792, 1988.